Neutral and negatively-charged formamide, N-methylformamide and dimethylformamide clusters

C. Desfrançois [a], V. Périquet [a], S. Carles [a], J.P. Schermann [a, *], L. Adamowicz [b]

[a] *Laboratoire de Physique des Lasers, Université Paris-Nord, 93430 Villetaneuse, France*
[b] *Chemistry Department, University of Arizona, Tucson, AZ 85721, USA*

Received 1 June 1998

Abstract

The structure and low energy electron attachment properties of small clusters of formamide, N-methylformamide and dimethylformamide have been studied. The experimental technique used is Rydberg electron transfer (RET) between laser-excited atoms and the molecular systems. The richness of hydrogen bonding possibilities of these three highly polar molecules leads to very different structures and resultant dipoles or quadrupoles which we determine by means of an empirical model. A corresponding wide variety of cluster anions is observed and interpreted, ranging from dipole-bound or quadrupole-bound anions in their ground state or first excited state to valence-type anions. © 1998 Elsevier Science B.V. All rights reserved.

1. Introduction

Formamide, N-methylformamide and dimethyl-formamide and their complexes are interesting for several reasons. For modeling proteins, they provide a simplified example of the peptide linkage and thus the structures of these molecules either isolated in the gas phase or in the condensed phase have been widely studied experimentally [1–3] as well as theoretically [4–12]. Hydrogen bonding is responsible for a large fraction of their physical and chemical properties and the replacement of hydrogen atoms by one or two methyl groups offers the possibility to modify the number of available H-bonds in the complexes. Another important property of these molecules is

their strong polarity. It has been recognized that eradication of tumors can be favoured by agents which induce differentiation of malignant cells and convert them in benign cells [13]. Among polar solvents which have an antitumor activity [14], N-methylformamide (NMF) plays an important role [15] and is more efficient than formamide (F) and dimethylformamide (DMF). The aim of this work is the experimental determination of the structures and electron attachment properties of the small homogeneous complexes of these three molecules in the gas phase. Each geometrical configuration of these polar complexes can be characterized by a total dipole moment which varies in a wide range, from zero in a head-to tail configuration up to more than 9 D in a linear chain. We thus take advantage of a well-suited ionization technique which introduces a nearly negligible perturbation of the nuclear geometries in contrast with conventional ionization processes. This

---

* Corresponding author. Tel.: +33-01-4940-3816; Fax: +33-01-4940-3200; E-mail scherman@lpl.univ-paris13.fr

ionization method derives from the possibility to bind an excess electron to a closed-shell molecule or cluster whose valence electron affinity is negative, provided its resultant dipole or quadrupole moment is larger than critical values $\mu_c = 2.5$ D for dipoles [16] and $Q_c = -40$ a.u. for negative quadrupoles or $Q_c = +35$ a.u. for positive quadrupoles [17]. An excess electron can then become very weakly bound by the long-range electron–dipole or electron–quadrupole field in a very diffuse orbital. A systematic means of production of such weakly bound anions is the use of laser-excited atoms which constitute a well-controlled source of very low energy electrons. The electron transfer collision rates are strongly dependent upon the respective energies of the exchanged electron in the excited atoms and in the accepting molecular system [18]. A first determination of the electron binding energies can thus be derived from the experimental measurement of the collisional anion formation rates. Since their excess electron binding energies are very small, typically in between 1 and 100 meV, external electric fields can detach the anions providing a second independant means of investigation of the molecular complexes. In the case of very weakly-bound excess electrons in complexes, we will here consider, in a first approximation, that the anions and their neutral parents have the same geometrical structures [19]. We will determine these structures by comparison of experimental results with the predictions of an empirical model.

2. Experimental results

2.1. Experimental techniques

Weakly-bound anions can be easily produced by transferring electrons from atoms highly excited in Rydberg states to polar or quadrupolar systems. The experimental technique has been described in detail in Ref. [20]. A pulsed beam of xenon atoms crosses at right angle a pulsed supersonic beam of molecules seeded in helium. Xenon atoms are first electron bombarded to produce metastable atoms which are further laser-excited towards selected Rydberg nf states in the collision region. The molecular cluster beam is produced by a heated (80–120°C) 0.15 mm

nozzle and passes downstream through a heated (100°C) 2 mm conical skimmer. Homogeneous neutral clusters are obtained by expanding few tens of mbar of molecular vapour mixed to 2 or 3 bar of helium. Ions created by charge exchange are extracted from the collision region and further accelerated into a time-of-flight mass spectrometer. We select principal Rydberg quantum numbers n from $n = 7$ to $n = 40$ and by comparison with SF_6^- signals due to collisions with a thermal effusive beam of SF_6 we deduce the n-dependencies of the rate constants for the formation of detected cluster anions. A set of three parallel mesh grids located in front of the channel plate detector and perpendicular to the ion path allows for the field detachment of the weakly bound anions. By setting a fourth grid to a highly repulsive negative voltage, we can measure the fraction of anions which has been neutralized [21]. A fraction of anions can already be neutralized by collisions with the residual gas (typically before reaching the field-detachment).

2.2. Rate constants for anion production

The mass spectra corresponding to the formation of cluster anions vary between the three different molecules. In the case of formamide, large $(F)_N^-$ anion signals are observed for $N = 1, 2, 3, 7$ and above. The tetramer, pentamer and hexamer anion signals are very weak and do not allow for quantitative measurements. The n-dependences of the monomer and trimer anion creation rates are both peaked at $n = 13$. The dimer anion also displays a peaked n-variation and tetramer anions are only observed at relatively low n-values around $n = 13$. Larger clusters $(N > 6)$ possess smooth n-dependences which do not fall to zero at large n-values and are thus characteristic of positive valence electron affinities [22]. Fig. 1 displays n-dependences of cluster anion creation rates and it is clearly seen in that the different cluster anions evolve more or less progressively from one type of behaviour to another one. In the following, we shall then consider a peaked n-dependence of the formation rate constants for a given anion as a signature of a weakly-bound electronic state with an excess electron in diffuse orbitals [18]. We have already shown in the case of
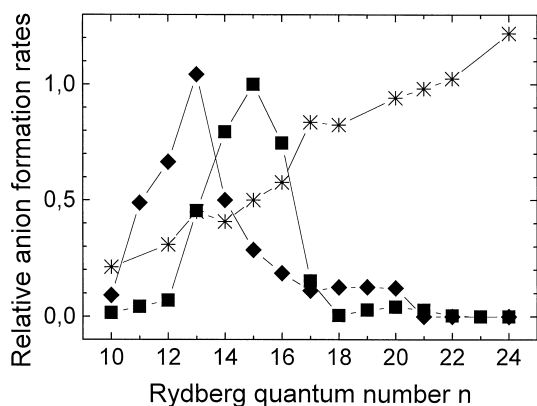
Fig. 1. Rydberg n-dependences of anion creation rates for the formamide dimer (squares), the formamide trimer (lozenges) and large $(F)_{N=7,8,9,10}^-$ formamide clusters (stars).

Fig. 2. Rydberg n-dependences of anion creation rates for the mixed formamide–N-methylformamide $(F\ldots NMF)^-$ dimer (circles) and the neat N-methylformamide $(NMF)_2^-$ dimer (triangles).

molecular dipole-bound or quadrupole-bound anions that a small dipole or quadrupole moment of parent neutrals qualitatively corresponds to a small electron binding energy and to a large n-value at which the formation rate constant is maximum [17]. The Rydberg selectivity of the anion production can be understood in the framework of a multiple crossing model [22] and an empirical law relates the excess electron binding energies EA to the value n_{max} at which the rate constants are maximum: EA (eV) = $23/n_{max}^{2.8}$.

For N-methylformamide, under the same experimental conditions as for formamide, we only observe the monomer and the dimer and no larger anion clusters. The n-dependences of the formamide, N-methylformamide (NMF) and dimethylformamide (DMF) monomer anions are similar, with only a small shift of the maximum for NMF towards larger n-values in between 13 and 14 and 14 for DMF. The n-dependence of the $(NMF)_2^-$ anion is displayed in Fig. 2. Over a smoothly varying background is superimposed a peak centered around $n = 25$. This striking difference between the homogeneous $(F)_2^-$ and $(NMF)_2^-$ anions prompted us to investigate the mixed $(F\ldots NMF)^-$ dimer anion. Its n-dependence displayed in Fig. 2 is a peaked curve characteristic of a weakly bound excess electron but broader than for the neat formamide dimer. With dimethylformamide, we only observe the monomer anion. This ensemble of observations will be interpreted with the help of calculations in Section 3.
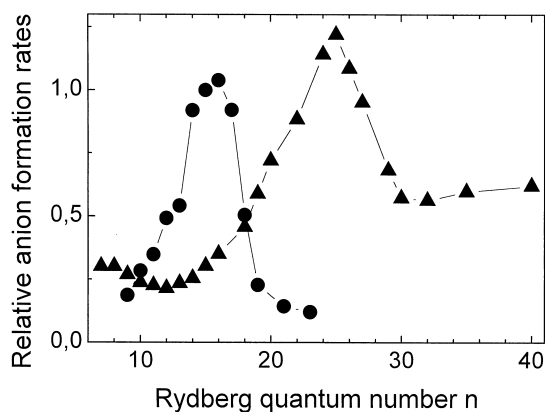
2.3. Field-detachment measurements

Fig. 3 displays field-detachment curves of the $(F)_2^-$ and $(NMF)_2^-$ dimer anions as well as the mixed $(F\ldots NMF)^-$ dimer anion. These field-detachment curves are obtained by measuring the fraction of electrically neutralized anions as a function of the externally applied electric field E to which they are submitted. It can be observed from Fig. 3 that a
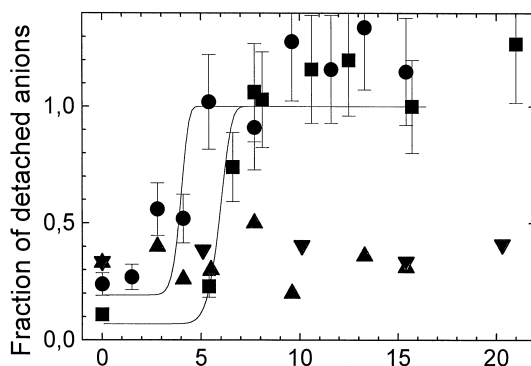

Fig. 3. Fraction of field-detached anions as a function of the detaching electric field. Squares correspond to the formamide dimer anion $(F)_2^-$, circles to the mixed formamide–N-methylformamide $(F\ldots NMF)^-$ dimer obtained from charge exchange with Xe(15f) Rydberg atoms. Up and down triangles correspond to N-methylformamide dimers respectively obtained from charge exchange with Xe(15f) and Xe(24f) Rydberg atoms. Lines correspond to best fits of experimental datas calculated with an electron tunnelling model (Ref. [22]) and respective electron affinities of 11 meV for $(F)_2$ and 8 meV for $(F\ldots NMF)$.

Dimer	Electron affinity (meV) n-dependence	Electron affinity (meV) Ryberg field-detachment
$(F)_2$	11.7	11
$F \ldots NMF$	9.7	8

fraction of anions has already been detached before reaching the field-detachment region. This has already been observed with our experimental set-up for a large number of weakly bound anions and may be attributed to collisional detachment along the anion path. Field-detachment is observed for $(F)_2^-$ and $(F \ldots NMF)^-$ by tuning the Rydberg quantum number at $n = 15$, but no field-detachment is observed for $(NMF)_2^-$ either at $n = 15$ or 25. By using a simple expression of the tunneling probability of the excess electron from a bound state to the free continuum [22], we can fit these experimental curves and obtain another independent determination of the excess electron binding energies EA (see Table 1) of $(F)_2^-$ and $(F \ldots NMF)^-$.

3. Neutral cluster structures and anion behaviours

3.1. Empirical model

In order to interpret the set of experimental results concerning the observations of anions and their different behaviours, we need the geometrical structures and the total dipoles of the neutral $(F)_N$, $(NMF)_N$ and $(DMF)_N$ complexes, and we use the following approach. We consider that weakly bound (dipole-bound or quadrupole-bound) anions possess excess electrons almost totally outside the molecular frame and exactly the same structures as their neutral parents. These structures are then calculated by means of an empirical model following the lines developed by No et al. [23]. The parameters of this model are chosen in order to reproduce as well as possible the dipole moments. The main advantage of such a simple model is that it requires a very limited amount

of computer time allowing for a complete exploration of the intermolecular potential energy surfaces. Moreover, the same set of parameters can be used for many molecular systems. However, the predictions concerning hydrogen-bonded complex geometrical structures and binding energies are only approximate and must thus be compared to experimental data.

We adopt for the total intermolecular potential energy only pair interactions, neglecting three-body and higher interactions [23,24]. The individual molecular geometries are frozen and the total intermolecular potential energy is expressed as a sum of Coulombic and Lennard-Jones or hydrogen-bond pair interaction terms V_{ij}, plus atomic polarization terms V'_{ij}:

$$V_{ij} = \frac{e^2}{4\pi\varepsilon_0} \frac{q_i q_j}{r_{ij}} + 4\varepsilon_{ij}\left\{\left(\frac{\sigma_{ij}}{r_{ij}}\right)^{12} - \left(\frac{\sigma_{ij}}{r_{ij}}\right)^{6}\right\} + \sum_i V'_i \tag{1}$$

where q_i or q_j are the partial charges located on atom i or j and ε_{ij} and σ_{ij} are the Lennard-Jones coefficients describing the interaction between atoms i and j. We adopt standard values for ε_{ii} and σ_{ii} [25] and obtain the mixed coefficients from the usual relationships: $\varepsilon_{ij} = \sqrt{\varepsilon_{ii}\varepsilon_{jj}}$ and $\sigma_{ij} = (\sigma_{ii} + \sigma_{jj})/2$. The atomic polarization terms are determined by means of the following expression:

$$V'_i = -2\pi\varepsilon_0\alpha_i\|\vec{E}_i\|^2 \tag{2}$$

where

$$\vec{E}_i = \sum_j \frac{q_j\vec{r}_{ij}}{r_{ij}^3}$$

is the electric field created by all the atomic charges of the neighbouring molecules and the atomic polarisabilities α_i are derived from standard bond polarisabilities.

In most empirical models, the adjustable parameters q_i, q_j are determined by least-square adjustments of the predictions of physical quantities, such as bond lengths, bond energies or spectral shifts [23], to the corresponding experimental values but in general do not lead to correct values of dipole and quadrupole moments. In this work, we focus our

attention on dipole and quadrupole binding of electrons and, we thus use partial charges q_i which we empirically determine in order to reproduce the experimental value of the known isolated molecular dipole moment of formamide, $\mu = 3.72$ D [25]. These partial charges are shown in Fig. 4. We then obtain respectively $\mu = 3.90$ D and $\mu = 3.23$ D for the *cis*-NMF and *trans*-NMF. The energy separation between these two configurations has been evaluated as equal to 52 meV by means of an ab initio (MP2) calculation and the corresponding respective populations are approximately 90 and 10% at room temperature, leading to a mean dipole moment of 3.83 D, close to the experimental values of 3.83 D [25] and 3.78 D [7]. The predicted value of the dipole of DMF is then 3.44 D, slightly less than the experimental value [25] of 3.8 D which is rather uncertain.

In order to take hydrogen bonds into account, we follow the lines of No et al. [23]. For each H-bond A–H . . . B–C, we multiply the non-bonded Lennard-Jones coefficients ε_{HB}, σ_{HB}, ε_{AB}, or ε_{HC}, σ_{AB} or σ_{HC} by respective bond dependent factors C, C', D and D' which we adjust to intermolecular binding energies of some well known hydrogen-bond

Table 2
van der Waals parameters used in the empirical model

Atom (function)	ε (meV)	σ (Å)
N (amide)	1.951	3.555
C (carbonyl)	6.115	3.332
O (carbonyl)	8.673	2.780
H_C (aliphatic)	1.605	2.601
H_N (amide)	2.689	2.388

dimers, e.g. $(H_2O)_2$, $(H_2O–NH_3)$, phenol(H_2O) and pyridine(H_2O) [26]. C and D' are larger than unity while C' and D are lower than 1 in order to obtain a deeper potential well, get a shorter H . . . B bond and to align the B–C bonds along the A–H bonds. The used parameters are given in Table 2. With the set of above described potential parameters, we use a home-made genetic algorithm in order to obtain the optimized complex geometries [27,28].

3.2. Formamide clusters

The replacement of hydrogen atoms by methyl groups strongly modifies the number of available H-bonds. While the individual dipoles of F, NMF
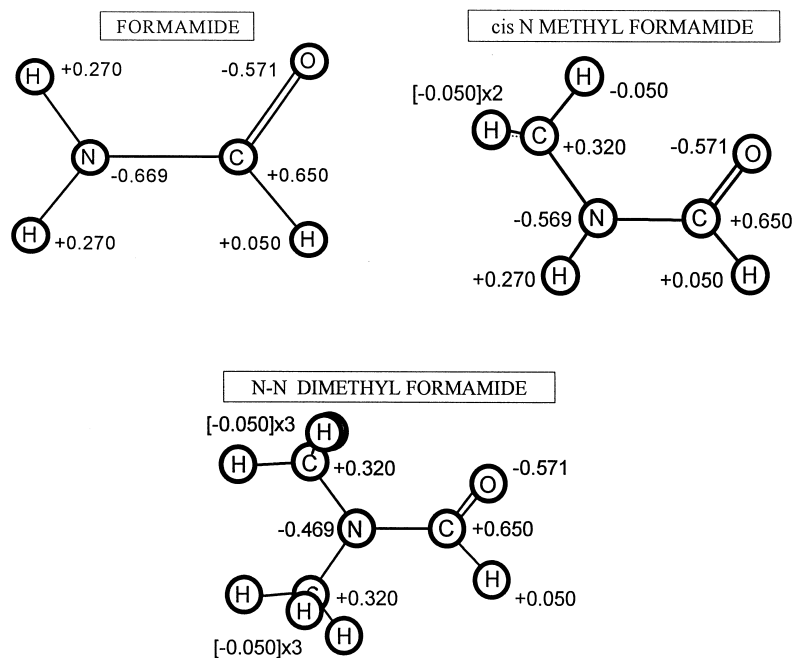
Fig. 4. Set of partial charges used in the empirical model (see text).

and DMF are relatively close, the structures of their clusters and thus the corresponding total dipoles are very different. The observation of the cluster anion behaviours (weak or strong electron binding) constitutes a direct test of the calculations.

The lowest energy configuration (A) of the neutral $(F)_2$ dimer has two H-bonds corresponding to a head-to-tail cyclic structure (Fig. 5) and thus a null dipole. Two configurations with large dipoles (B and C) lying several hundreds of meV above cannot be populated in the cluster beam and thus cannot be held as parents of the observed loosely bound anions (Table 3). The neutral $(F)_2$ dimer has a large quadrupole moment of $+36$ a.u. and the observation

Table 3
Predictions of the empirical calculations concerning the properties of the neutral formamide dimer

Formamide dimer configuration	A	B	C
Energy (meV)	0	225	227
Binding energy ab initio [9]	479–609		
Empirical (present work) (meV)	606	381	379
Dipole moment (D)	0	5.97	8

of $(F)_2^-$ can thus be interpreted as a proof for the existence of quadrupole-bound cluster anions.

The lowest energy configuration of the $(F)_3$ neutral cluster is a monomer unit strongly bound to a cyclic dimer by two H-bonds (Fig. 5). This situation is rather usual in polar systems such as acetonitrile [19]. From the point of view of anion formation, the trimer behaviour is very close to that of the monomer. Its calculated (empirical) binding energy and dipole moment are respectively 1185 meV and 3.82 D, in good agreement with the observation of an anion with a weakly bound excess electron (17.2 meV). The formamide neutral tetramer (Fig. 5) is formed by two H-bonds linking of two cyclic dimers. Its empirically calculated binding energy, dipole and quadrupole moments are respectively equal to 1826 meV, 0.03 D and 65.6 a.u. This very large value of the quadrupole moment is consistent with the observation of $(F)_4^-$ anion signals at low n-values in the vicinity of $n = 13$ suggesting a possible quadrupole-bound anion state but the weakness of the signals does not allow us to draw quantitative conclusions.

When the cluster size increases, the well-known solvation effect induces stabilization of the anions with respect to their neutral parents. The pentamer and hexamer anions are barely observable at some n-values but above a size threshold of 7 formamide molecules, a valence-type behaviour appears in the RET curve (Fig. 1) corresponding to the creation of solvated anions. We have previously measured cluster size thresholds for observation of valence anions created by Rydberg electron attachment to polar molecules with known negative electron affinities [29]. By comparison with those other polar systems, the observation of the formamide threshold provides us a rough estimation of the negative valence electron affinity of the formamide monomer equal to -1 (0.4) eV.
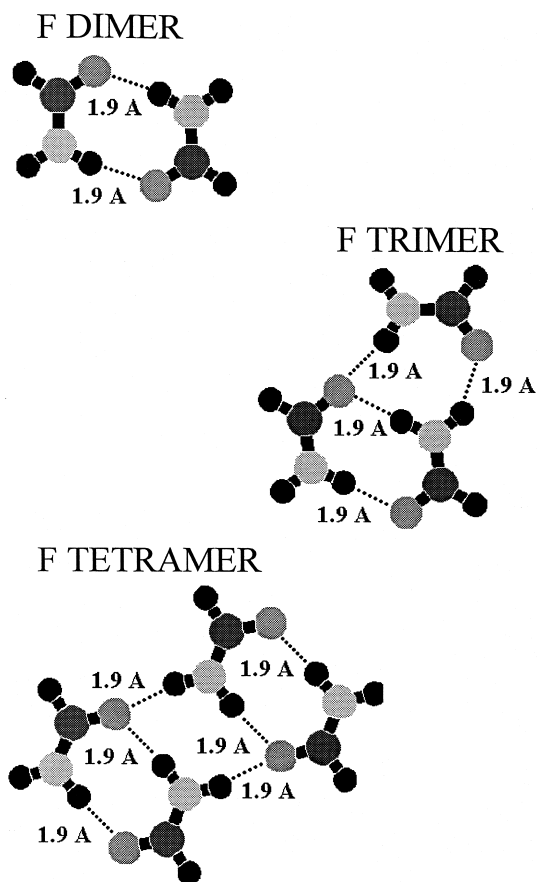

Fig. 5. Geometrical structures of the lowest energy configurations of the neutral formamide dimer, trimer and tetramer predicted by the empirical model. These three configurations are planar. Labelling of atoms is given in Fig. 6.

3.3. N-Methylformamide clusters

The intermolecular binding energies and the corresponding dipole moments of the lowest energy configurations of the NMF dimer calculated by means of the empirical model are given in Table 4. The structure of the lowest energy configuration of this dimer is displayed in Fig. 6. NMF is interesting because its monomer can adopt two configurations which are energetically close. As stated above, we can evaluate that 85% of the monomer molecules are in the *cis* configuration and 15% in the *trans* configuration at the temperature of the stagnation chamber producing the cluster beam. If absolutely no thermalization was taking place in the clustering region of the beam, we would expect relative populations of the *trans–trans*, *cis–cis* and *cis–trans* dimer configurations respectively equal to 2, 72 and 26%. From the intermolecular binding energies and the relative energies of the two NMF isomers, we have calculated the relative energies of the dimers (Table 4). Energetically, the most stable is the *trans–trans* cyclic dimer with two H-bonds and a null dipole. The *cis–cis* and the *cis–trans* dimers respectively lie 84 and 125 meV above the *trans–trans* dimer. The final dimer populations in the RET collision region depend on the initial populations and the thermalization in the cluster beam. The temperature of the clustering valve is around 370 K and adiabatic cooling brings the beam temperature down to 100–150 K [19]. Since dimers are produced in the early region of the clustering beam, we take a Boltzmann distribution at a mean value of 300 K and we obtain as very crude estimation of the respective relative final populations equal to 26, 71 and 3%. The *trans–trans* dimer configuration would have led to the observation of field-detachable quadrupole-bound anions in contradiction with the experiment. We interpret the experimental observation of the smoothly-varying background of the Rydberg n-dependence of the $(NMF)_2^-$ anion creation rate as due to electron attachment to the majority of the dimers which are formed as *cis–cis* (A) dimers. This metastable *cis–cis* dimer possesses an extremely large dipole moment of 8.5 D as compared to usual molecular systems leading to ground state dipole or quadrupole-bound anions, typically in between 2.5 and 5 D [17,18]. This dimer thus leads to the formation of an anion whose excess electron possess a binding energy in the same range (≈ 1 eV) as alkali halides [16,30]. It is known [31] that molecular systems with large dipoles can lead to dipole-bound anions possessing electronically excited states. Photodetachment studies of cyanomethyl or acetaldehyde enolate anions [32] have demonstrated the existence of these excited states. The presence of a peak around $n = 25$ suggests the possibility of electron attachment into the first excited state of the dipole-bound anion. The electron binding energy in this state would then be equal approximately to 2.8 meV. If this interpretation is correct, the fact that we cannot field-detach such a weakly bound excess electron may be due to a strong coupling between the excited state responsible for the attachment process and the strongly-bound ground state. A similar situation is observed in nitromethane where the Rydberg electron attachment behaviour is dominated by the dipole state which is strongly coupled to the valence state [33].

In absence of *cis–trans* isomerisation in the beam, the N-methylformamide trimer formed by clustering of molecules in their most stable configuration is the $(cis\text{-}NMF)_3$ cluster which has a binding energy of 1060 meV and a dipole moment of 0.36 D. This result is experimentally confirmed since, in contrast with formamide, the corresponding trimer anion is

Table 4
Predictions of empirical calculations concerning the properties of the neutral N-methylformamide dimers. The origin of energies is the energy of the *trans–trans* dimer

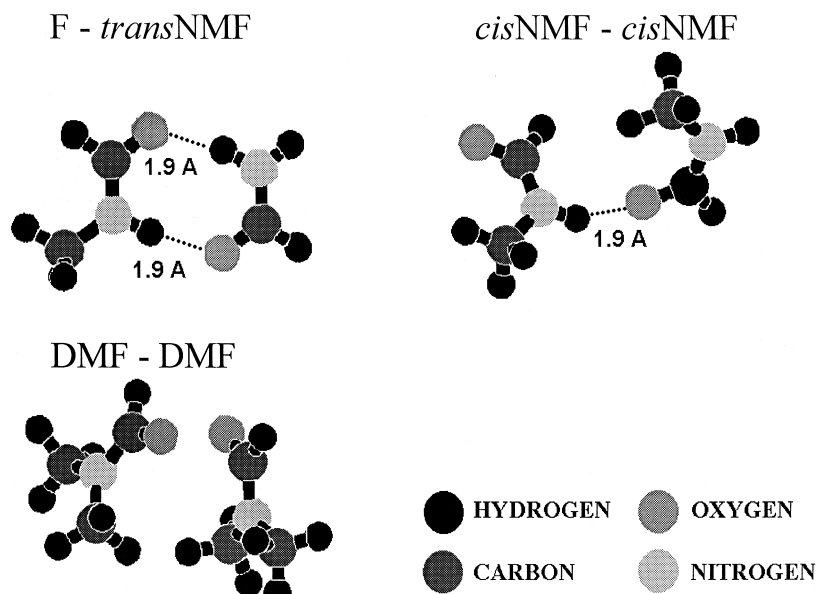| N-Methylformamide dimer configuration	*trans–trans*	*cis–trans*	*cis–cis* (A)	*cis–cis* (B)
Energy (meV)	0	210	230	370
Binding energy (meV)	642	465	454	379
Dipole moment (D)	0	1.55	8.54	0

Fig. 6. Geometrical structures of the lowest energy configurations of the neutral (*cis*-NMF–*cis*-NMF), (F–*trans*-NMF) and (DMF–DMF) dimers predicted by the empirical model.

not observed, as well as the $(cis\text{-NMF})_4$ tetramer which has a binding energy of 1827 meV and a dipole moment of 0.1 D.

3.4. Mixed formamide–N-methylformamide dimer

The Rydberg *n*-dependence of the rate constant for the formation of the mixed $(F\ldots NMF)^-$ dimer anion exhibits a broad peak around $n = 16$ (Fig. 2). In contrast with the $(NMF)_2^-$ anion, this mixed dimer is field-detachable (Fig. 3). We have also calculated the relative energies of the neutral $(F\ldots cis\text{-NMF})$ and $(F\ldots trans\text{-NMF})$ dimers. The *cis* configuration lies 130 meV above the *trans* configuration. An analysis of the cluster beam composition similar to the above described in the case of the NMF dimers lead us to respective populations of 5 and 95% for the *cis* and *trans* configurations. The structure of the neutral $(F\ldots cis\text{-NMF})$ in its lowest energy configuration is displayed in Fig. 6 and has a low dipole of only 1.54 D. It cannot thus be held as parent of the observed anion. Two higher lying configurations have dipoles of 6.4 and 8.5 D would have led to strongly bound anions. We thus consider the mixed $(F\ldots NMF)^-$ dimer anion as a quadrupole-bound anion due to electron attachment to the most popu-

lated $(F\ldots cis\text{-NMF})$ configuration similar to the neat $(F)_2^-$.

3.5. Dimethylformamide clusters

Except for the monomer, we do not observe any anion with dimethylformamide. The presence of two methyl groups in DMF forbids the formation of cyclic dimers. The empirical calculation provides two pairs of low lying configurations with respective dipole moments and binding energies equal to 1.2 D (345 meV) and 0.2 D (320 meV), 3.7 D (300 meV) and 4.8 D (295 meV). The geometry of the lowest energy configuration is displayed in Fig. 6. The first pair of these configurations have much too low total dipoles to allow for dipole-bound anions and it is unlikely that the second pair of configurations is populated in the cluster beam. These predictions are thus in agreement with the experimental observations.

4. Conclusion

A large variety of anions can be obtained by electron attachment to the clusters of three rather

similar molecules F, NMF and DMF. Most interesting is the presence within the same molecular systems of new weakly bound anions which have been predicted for a long time but never observed, such as quadrupole-bound anions or excited states of dipole-bound anions. With the same set of a rather small number of empirical parameters, we have been able to calculate the geometrical structures of the different neutral clusters and to fully interpret the different anion behaviours. The approach of involving weak dipole-type binding for the interpretation of negative ion mass spectra of polar systems [19] appears here extendable to systems with zero dipole moments, but sufficiently large quadrupoles. Many small molecules of biological interest such as DNA bases or amino acids have large dipoles and/or large quadrupoles. The above demonstrated method can be used for studying their interactions in gas phase and directly compare to elaborate quantum chemistry calculations.

References

[1] Y. Sugawara, Y. Hamada, A.Y. Hirakawa, M. Tsuboi, Chem. Phys. Lett. 67 (1979) 186.

[2] F.J. Lovas, R.D. Suenram, G.T. Fraser, G.W. Gillies, J. Zozom, J. Chem. Phys. 88 (1988) 722.

[3] (a) S. Nasr, L. Bosio, J. Chem. Phys. 108 (1998) 2297; (b) M.C. Bellissent-Funel, S. Nasr, L. Bosio, J. Chem. Phys. 106 (1997) 7913.

[4] P. Boui, C.N. Tam, J. Sopkova, F.R. Trouw, J. Chem. Phys. 108 (1998) 351.

[5] G. Fogarasi, A. Balazs, J. Mol. Struct. (Theochem.) 133 (1985) 105.

[6] P.-O. Astrand, G. Karlstroem, A. Engdahl, B. Nelander, J. Chem. Phys. 102 (1995) 3524.

[7] A.C. Fantoni, W. Caminati, J. Chem. Soc. Faraday Trans. 92 (1996) 343.

[8] N. Sathyan, V. Santhanam, J. Sobhanadri, J. Mol. Struct. (Theochem.) 333 (1995) 179.

[9] P. Hobza, J. Sponer, J. Mol. Struct. (Theochem.) 388 (1996) 115.

[10] W. Chen, M.S. Gordon, J. Chem. Phys. 105 (1996) 11081.

[11] R. Ludwig, F. Weinhold, T.C. Farrar, J. Chem. Phys. 107 (1997) 500.

[12] S.A. Cooke, G.K. Corlett, C.M. Evans, A.C. Legon, J.H. Holloway, J. Chem. Phys. 108 (1998) 39.

[13] E.N. Gate, J. Med. Chem. 29 (1986) 1046.

[14] (a) E.N. Spremulli, D.L. Dexter, J. Clin. Oncol. 2 (1984) 227; (b) N. Motohashi, Anticancer Res. 17 (1997) 3431.

[15] I. D'Agnano, V. Turchi, M. Nuti, C. Leonetti, G. Zupi, Cell Prolif. 25 (1992) 299.

[16] C. Desfrançois, H. Abdoul-Carime, N. Khelifa, J.P. Schermann, Phys. Rev. Lett. 73 (1994) 2436.

[17] H. Abdoul-Carime, C. Desfrançois, Eur. Phys. J. D., in press.

[18] C. Desfrançois, H. Abdoul-Carime, J.P. Schermann, Int. J. Mod. Phys. B 10 (1996) 1339.

[19] C. Desfrançois, H. Abdoul-Carime, N. Khelifa, J.P. Schermann, V. Brenner, P. Millié, J. Chem. Phys. 102 (1995) 4952.

[20] C. Desfrançois, H. Abdoul-Carime, C. Adjouri, N. Khelifa, J.P. Schermann, Europhys. Lett. 26 (1994) 25.

[21] C. Desfrançois, B. Baillon, J.P. Schermann, S.T. Arnold, J.H. Hendricks, K.H. Bowen, Phys. Rev. Lett. 72 (1994) 48.

[22] C. Desfrançois, Phys. Rev. A 51 (1995) 3667.

[23] K.T. No, O.Y. Kwon, S.Y. Kim, M.S. Jhon, H.A. Scheraga, J. Phys. Chem. 99 (1995) 3478.

[24] J.A. Fernandez, E.R. Bernstein, J. Chem. Phys. 106 (1997) 3029.

[25] D.R. Lide, in CRC Handbook of Chemistry and Physics, 74th edn., CRC Press, Boca Raton, FL.

[26] H. Abdoul-Carime, A. Wakisaka, Y. Bouteiller, C. Desfrançois, J.P. Schermann, Z. Phys. D 40 (1997) 55.

[27] Y. Zeiri, Phys. Rev. 51E (1995) 2769.

[28] H. Abdoul-Carime, A. Wakisaka, J. Flugge, H. Takeo, V. Periquet, J.P. Schermann, C. Desfrançois, J. Chem. Soc. Faraday Trans. 93 (1997) 4289.

[29] C. Desfrançois, H. Abdoul-Carime, N. Khelifa, J.P. Schermann, J. Chim. Phys. 92 (1995) 409.

[30] T. Miller, D.G. Leopold, K.K. Murray, W.C. Lineberger, J. Chem. Phys. 87 (1987) 1549.

[31] W.R. Garrett, J. Chem. Phys. 73 (1980) 5721.

[32] A.H. Zimmerman, J.I. Brauman, J. Chem. Phys. 66 (1977) 5823.

[33] R.N. Compton, H.S. Carman, C. Desfrançois, H. Abdoul-Carime, J.P. Schermann, J.H. Hendricks, S.A. Lyapustina, K.H. Bowen, J. Chem. Phys. 105 (1996) 3472.